molecular pharmaceutics

Article

pubs.acs.org/molecularpharmaceutics

PEG-Farnesyl Thiosalicylic Acid Telodendrimer Micelles as an Improved Formulation for Targeted Delivery of Paclitaxel

Xiaolan Zhang,[†,‡,§] Yixian Huang,[†,‡,§] Wenchen Zhao,[‡] Yichao Chen,[†,‡,§] Peng Zhang,[†,‡,§] Jiang Li,[†,‡,§] Raman Venkataramanan,[‡] and Song Li*[,†,‡,§]

[†]Center for Pharmacogenetics, [‡]Department of Pharmaceutical Sciences, School of Pharmacy, and [§]University of Pittsburgh Cancer Institute, University of Pittsburgh, Pittsburgh, Pennsylvania 15261, United States

Supporting Information

ABSTRACT: We have recently designed and developed a dual-functional drug carrier that is based on poly(ethylene glycol) (PEG)-derivatized farnesylthiosalicylate (FTS, a nontoxic Ras antagonist). PEG_{5K}-FTS_2 readily form micelles (20−30 nm) and hydrophobic drugs such as paclitaxel (PTX) could be effectively loaded into these micelles. PTX formulated in PEG_{5K}-FTS_2 micelles showed an antitumor activity that was more efficacious than Taxol in a syngeneic mouse model of breast cancer (4T1.2). In order to further improve our PEG-FTS micellar system, four PEG-FTS conjugates were developed that vary in the molecular weight of PEG (PEG_{2K} vs PEG_{5K}) and the molar ratio of PEG/FTS (1/2 vs 1/4) in the conjugates. These conjugates were characterized including CMC, drug loading capacity, stability, and their efficacy in delivery of anticancer drug PTX to tumor cells *in vitro* and *in vivo*. Our data showed that the conjugates with four FTS molecules were more effective than the conjugates with two molecules of FTS and that FTS conjugates with PEG_{5K} were more effective than the counterparts with PEG_{2K} in forming stable mixed micelles. PTX formulated in PEG_{5K}-FTS_4 micelles was the most effective formulation in inhibiting the tumor growth *in vivo*.

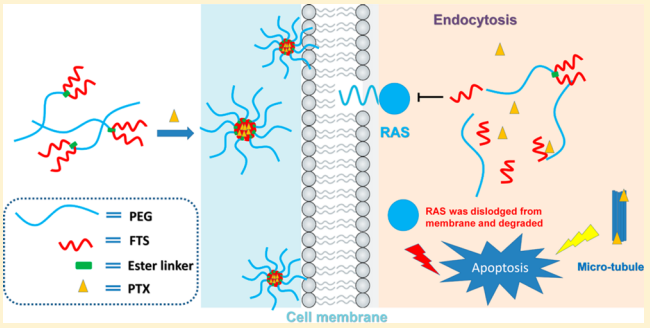

KEYWORDS: *paclitaxel, farnesyl thiosalicylic acid, dual function, nanomicelles, targeted delivery*

INTRODUCTION

Paclitaxel (PTX) is one of the first-line chemotherapeutics used to treat patients with breast, ovarian, nonsmall cell lung cancer, and advanced forms of Kaposi's sarcoma. The mechanism involves interfering with the normal breakdown of microtubules during cell division.[1] Successful application of PTX in the clinic has been limited by its poor water solubility and the systemic toxicity. Taxol is a Cremophor EL/ethanol formulation of PTX that has been used in the clinic. However, Cremophor EL can cause hyperactivity reactions, neuropathy, and other serious side effects.[2] Thus, there is a need to develop an alternative delivery system for PTX. Various macromolecular delivery systems such as liposomes, dendrimers, and nanoparticles are under investigation, among which polymeric micelles have gained considerable attention owing to ease in preparation and their very small sizes (10−100 nm).[3−7] Recent studies have substantiated that sub-100 nm was critical for a delivery system to achieve effective tumor targeting.[8−13]

Our group has previously developed PEG-FTS as a dual-functional carrier for the delivery of poorly water-soluble anticancer drugs.[14] This system was constructed by coupling two molecules of *S-trans,trans*-farnesylthiosalicylic acid (FTS) to poly(ethylene glycol) (PEG, M_W = 5000) through an ester linkage (PEG_{5K}-FTS_2). Different from most reported delivery systems that use "inert" excipients, our system employ water-insoluble drug FTS as the hydrophobic region of polymeric micelles. FTS is a nontoxic Ras antagonist.[15−17] It can inhibit both oncogenically activated Ras and growth factor receptor-mediated Ras activation, resulting in the inhibition of Ras-dependent tumor growth.[18−21] Preliminary study showed that the antitumor activity of FTS was well retained following coupling to PEG_{5K}. Furthermore, PEG_{5K}-FTS_2 readily formed small-sized micelles (20−30 nm) that are effective in loading and delivering PTX. *In vivo* study demonstrated that the antitumor activity of the PTX-loaded PEG_{5K}-FTS_2 micelles was significantly higher than that of Taxol.[14]

Recent studies from us and others have shown that the Vitamin E-based micellar system could be significantly improved via modulating the PEG motifs and the molar ratio of PEG/Vitamin E.[22−24] In another study with PEG-embelin system, we showed that a conjugate with two embelin molecules linked to PEG was significantly more effective than the conjugate with one embelin molecule coupled to PEG.[25,26] This has prompted us to carry out a similar study with PEG-FTS system. Four PEG-FTS conjugates that vary in the

Received: March 5, 2014
Revised: April 25, 2014
Accepted: July 2, 2014
Published: July 2, 2014

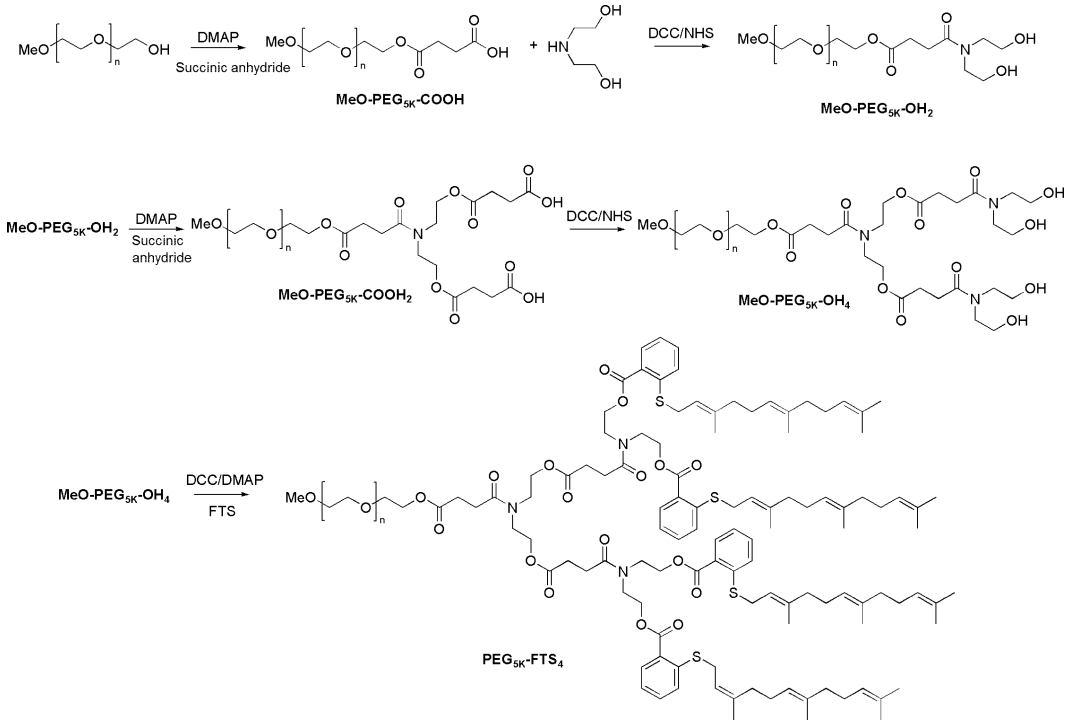

Figure 1. Synthesis scheme of PEG_{5K}-FTS_4 conjugate.

molecular weight of PEG (PEG_{2K} vs PEG_{5K}) and the molar ratio of PEG/FTS (1/2 vs 1/4) have been developed. We demonstrated that PEG_{5K}-FTS_4 formed the most stable mixed micelles with PTX among the four PEG-FTS conjugates. Furthermore, PTX formulated in PEG_{5K}-FTS_4 micelles was the most effective formulation in inhibiting the tumor growth *in vivo*.

EXPERIMENTAL SECTION

Materials. Paclitaxel (98%) was purchased from AK Scientific Inc. (CA, U. S. A.). FTS was synthesized and purified following a published literature.[27] Dulbecco's phosphate buffered saline (DPBS) was purchased from Lonza (MD, U. S. A.). Poly(ethylene glycol) methyl ether (MeO−PEG−OH, M_W = 2000, 5000 kDa), dimethyl sulfoxide (DMSO), succinate anhydride, diethanolamine, 3-(4,5-dimethylthiazol-2-yl)-2,5-diphenyl tetrazolium bromide (MTT), trypsin-EDTA solution, Triton X-100, and Dulbecco's Modified Eagle's Medium (DMEM) were all purchased from Sigma-Aldrich (MO, U. S. A.). Fetal bovine serum (FBS) and penicillin−streptomycin solution were purchased from Invitrogen (NY, U. S. A.). *N*-hydroxysuccinimide (NHS) and dicyclohexylcarbodiimide (DCC) were purchased from Alfa Aesar (MA, U. S. A.). 4-(dimethylamino) pyridine (DMAP) was purchased from Calbiochem-Novabiochem Corporation (CA, U. S. A.). All solvents used in this study were HPLC grade.

Cell Culture. MCF-7 is human breast carcinoma cell line. 4T1.2 is a mouse metastatic breast cancer cell line. HCT-116 is a human colon carcinoma cell line. All cell lines were cultured in DMEM containing 5% FBS and 1% penicillin-streptomycin at 37 °C in a humidified 5% CO_2 atmosphere.

Synthesis of PEG_{2K}-FTS_2, PEG_{2K}-FTS_4, PEG_{5K}-FTS_2, and PEG_{5K}-FTS_4. PEG_{5K}-FTS_4 was prepared via solution phase condensation reactions (Figure 1). We started to synthesize two hydroxyl group terminated PEG monomethyl ether (MeO−PEG_{5k}−OH_2) following the literature.[10] Carboxyl terminated PEG monomethyl ether (MeO−PEG_{5k}−$COOH_2$) was synthesized from MeO−PEG_{5k}−$(OH)_2$ by a facile chemical reaction with succinic anhydride and DMAP. To obtain four hydroxyl groups terminated PEG monomethyl ether (MeO−PEG_{5k}−OH_4), diethanolamine was coupled onto the carboxylic group of MeO−PEG_{5k}−$COOH_2$ using NHS/DCC as coupling agent in chloroform overnight. The polymer was precipitated and washed by ice-cold diethyl ether and ethanol twice, respectively, and concentrated under vacuum. MeO−PEG_{5k}−OH_4, FTS, DCC, and DMAP were then dissolved in chloroform and allowed to react overnight at room temperature. The solution was filtered and precipitated in ice-cold diethyl ether and ethanol twice respectively, and concentrated under vacuum. The powder was then dissolved in water and filtered through a filter with a pore size of 0.22 μm. The final product was obtained by lyophilizing the filtrate. PEG_{2K}-FTS_4 was similarly synthesized as PEG_{5K}-FTS_4. PEG_{5K}-FTS_2 and PEG_{2K}-FTS_2 were synthesized following the literature.[16]

Preparation of Drug-Loaded and Drug-Free Micelles. PTX (10 mM in chloroform) and four PEG-FTS conjugates (10 mM in chloroform) were mixed at various carrier/drug ratios. The organic solvent was removed by nitrogen flow to form a thin film of drug/carrier mixture. The film was dried under vacuum for 1 h to remove the remaining solvent. DPBS was added to hydrate the thin film and the drug-loaded micelles were formed. Unincorporated PTX (precipitate) was removed by filtering through a syringe filter (pore size: 0.22 μm). The drug-free micelles were similarly prepared as described above.

Characterizations of Drug-Loaded and Drug-Free Micelles. The particle size and zeta potential of micelles were measured by a Zetasizer (DLS) (Zetasizer Nano ZS instrument, Malvern, Worcestershire, U. K.). The morphology and size distribution of drug-free or drug-loaded PEG_{2K}-FTS_2, PEG_{2K}-FTS_4, PEG_{5K}-FTS_2, and PEG_{5K}-FTS_4 micelles were

dx.doi.org/10.1021/mp500181x | *Mol. Pharmaceutics* 2014, 11, 2807−2814

observed using transmission electron microscopy (TEM). A copper grid with Formvar was used. The copper grid was immersed in a drop of sample solution and stained with 1% uranyl acetate. Imaging was performed at room temperature on JEOL JEM-1011.

The critical micelle concentrations (CMC) of four PEG-FTS micelles were determined by using pyrene as a fluorescence probe.[28] Four PEG-FTS conjugates, PEG_{2K}-FTS_2, PEG_{2K}-FTS_4, PEG_{5K}-FTS_2, and PEG_{5K}-FTS_4, were prepared in chloroform at 1.2 mg/mL, and various amounts were added to nine separate vials. Then 10 μL of 1.8×10^{-4} M of pyrene in chloroform was added to each vial and the solution was mixed well. The organic solvent was removed by oil pump, and then 3 mL of Milli-Q water was added to each vial. The final pyrene concentration was 6×10^{-7} M with the four PEG-FTS conjugate concentrations ranging from 0.0001 to 0.5 mg/mL. The vials were kept on a shaker for 24 h at 37 °C to reach equilibrium before fluorescence measurement. The fluorescence intensities of samples were measured at the excitation wavelength of 334 nm and emission wavelength of 390 nm by Synergy H1 Hybrid Multi-Mode Microplate Reader (Winooski, VT, U. S. A.). The CMC is determined from the threshold concentration, where the sharp increase in pyrene fluorescence intensity is observed.

The PTX loading efficiency was quantified by high performance liquid chromatography (HPLC) (Alliance 2695-2998 system) as described previously.[16] Drug loading capacity (DLC) and drug loading efficiency (DLE) were calculated according to the following equation:

$$\text{DLC}\ (\%) = \frac{\text{weight of drug loaded}}{\text{weight of polymer} + \text{drug used}} \times 100\%$$

$$\text{DLE}(\%) = \frac{\text{weight of loaded drug}}{\text{weight of input drug}} \times 100\%$$

***In Vitro* PTX Release Study.** The *in vitro* PTX release kinetics for the four PEG-FTS micelles was determined by a dialysis method according to our published protocol.[14] Briefly, PTX loaded PEG-FTS micelles at a concentration of 0.5 mg PTX/mL were placed into a dialysis bag (M_W cutoff 14000). The dialysis bag was incubated in 200 mL PBS containing 0.5% (w/v) Tween 80 with gentle shaking at 37 °C. The concentrations of PTX remaining in the dialysis bag at designated time points were measured by HPLC.

Hemolytic Effect of PEG-FTS Micelles. Hemolysis assay was performed using fresh blood collected through cardiac puncture from rats.[29] Red blood cells (RBCs) were collected by centrifugation and washed with PBS three times. Then RBCs were diluted in PBS with a final concentration of 2% w/v. A total of 1 mL of diluted RBC suspension was mixed with different concentrations (0.2 and 1.0 mg/mL) of four PEG-FTS micelles and PEI, respectively, and then incubated at 37 °C in an incubator shaker for 4 h. The mixtures were centrifuged, and supernatants were transferred into a 96-well plate. The release of hemoglobin was determined at 540 nm absorbance using a microplate reader. RBCs incubated with PBS and Triton X-100 (2%) were used as the negative and positive controls, respectively. The percentage of hemolysis of RBCs was calculated as $(OD_{sample} - OD_{negative\ control})/(OD_{positive\ control} - OD_{negative\ control}) \times 100\%$.

***In Vitro* Cytotoxicity Study.** The cytotoxicity of PTX formulated in PEG_{2K}-FTS_2, PEG_{2K}-FTS_4, PEG_{5K}-FTS_2, and PEG_{5K}-FTS_4 micelles was assessed with several cancer cell lines and compared to free PTX in DMSO, respectively. Briefly, 4T1.2 (1000 cells/well) cell lines were seeded in 96-well plates. After 24 h of incubation in DMEM with 5% FBS and 1% streptomycin−penicillin, the old medium was removed and the cells were incubated for 72 h in the presence of indicated concentrations of PTX (free or formulated in four PEG-FTS micelles). A total of 100 μL of 3-(4,5-dimethylthiazol-2-yl)-2,5-diphenyltetrazolium bromide (MTT) in DPBS (0.5 mg/mL) was added to each well and cells were further incubated for 2 h. MTT formazan was solubilized by DMSO. The absorbance in each well was measured by a microplate reader with wavelength at 550 nm and reference wavelength at 630 nm. Untreated groups were used as controls. Cell viability was calculated as $[(OD_{treat} - OD_{blank})/(OD_{control} - OD_{blank}) \times 100\%]$. The cytotoxicity of PEG_{2K}-FTS_2, PEG_{2K}-FTS_4, PEG_{5K}-FTS_2, and PEG_{5K}-FTS_4 micelles alone was similarly tested in 4T1.2, MCF-7, and HCT-116 cell line as described above.

Western Blotting. Ras protein expression level in HCT-116 cells was evaluated by Western blotting following our published method.[14] Briefly, HCT-116 cells with 60−70% confluency in a 6-well plate were treated with four PEG-FTS conjugates for 20 h at a FTS concentration of 40 μM. The antibodies used for Western blotting included those against Ras and β-actin. Bound antibodies were detected by chemiluminescence.

Animals. Female BALB/c mice, 4−6 weeks in age, were purchased from Charles River (Davis, CA, U. S. A.). All animals were housed under pathogen-free conditions according to AAALAC guidelines. All animal-related experiments were performed in full compliance with institutional guidelines and approved by the Animal Use and Care Administrative Advisory Committee at the University of Pittsburgh.

***In Vivo* Therapeutic Study.** A syngeneic murine breast cancer model (4T1.2) was used to examine the therapeutic effect of different formulations of PTX. A total of 2×10^5 4T1.2 cells in 200 μL of PBS were inoculated s.c. at the right flank of female BALB/c mice. Treatments were started when tumors in the mice reached a tumor volume of ~50 mm^3 and this day was designated as day 1. On day 1, these mice were randomly divided into six groups ($n = 5$) and administered i.v. with PBS (control), Taxol (10 mg PTX/kg), PTX-loaded PEG_{2K}-FTS_2, PEG_{2K}-FTS_4, PEG_{5K}-FTS_2, and PEG_{5K}-FTS_4 micelles (10 mg of PTX/kg), respectively on days 1, 3, 5, 8, 10, and 12. Tumor sizes were measured with digital caliper three times a week and calculated by the formula: $(L \times W^2)/2$, where L is the longest and W is the shortest of the tumor diameters (mm). To compare between groups, relative tumor volume (RTV) was calculated at each measurement time point (where RTV equals to the tumor volume at a given time point divided by the tumor volume prior to first treatment). Mice were sacrificed before the tumor reached 2000 mm^3.

To monitor the potential toxicity, the body weights of all mice from different groups were measured every three days. In addition, serum levels of transaminases (AST, ALT) in the mice with different treatments were investigated at the completion of the study.

Statistical Analysis. In all statistical analysis, the significance level was set at a probability of $P < 0.05$. All results were reported as the mean ± standard deviation (SD). unless otherwise indicated. Statistical analysis was performed by Student's t test for two groups, and one-way ANOVA for multiple groups, followed by Newman−Keuls test if $P < 0.05$.

RESULTS

Synthesis of Four PEG-FTS Conjugates. PEG_{5K}-FTS_4 conjugate, containing four molecules of FTS coupled to one molecule of PEG_{5K} via a labile ester linkage, was developed by solution phase condensation reactions. The synthetic scheme is presented in Figure 1. ^1H NMR spectra of PEG_{5K}-FTS_4 conjugate are shown in Supporting Information Figure S1D. The intense peak at 3.66 ppm was attributable to the methylene protons of PEG. Carbon chain signals and benzene ring signals of FTS were located at 1.5−2.2 ppm and 7−8 ppm, respectively. MALDI-TOF suggested that four FTS were successfully attached to PEG_{5K} (Supporting Information Figure S2D). We also synthesized PEG_{2K}-FTS_2, PEG_{2K}-FTS_4, and PEG_{5K}-FTS_2 conjugates, which were confirmed by ^1H NMR spectra and MALDI−TOF mass spectra (Supporting Information Figures S1 and S2).

Size and Size Distribution of Micelles. The four PEG-FTS conjugates readily formed micelles in aqueous solution with the particle sizes of 20−30 nm (Table 1). Dynamic light scattering (DLS) measurements showed that PEG_{5K}-FTS_4 micelles had hydrodynamic sizes around 27 nm at the concentration of 20 mg/mL (Figure 2A). TEM revealed spherical particles with uniform size distribution (Figure 2B). The size observed by TEM shows good agreement with that determined by DLS (Supporting Information Figures S3 and S4). PTX could be effectively loaded into PEG_{5K}-FTS_4 micelles. The spherical shape and size distribution were well retained when PTX was loaded into micelles at a drug concentration of 1 mg/mL and a carrier/drug ratio of 2.5/1 (m/m) (Figure 2C and Figure 2D). Similar results were shown for the other three micelles (Supporting Information Figures S3 and S4).

Table 1. Size and CMC of Four PEG-FTS Conjugates

conjugates	size[a]	PDI[b]	CMC[c] (μM)
PEG_{2K}-FTS_2	25.75	0.09	1.22
PEG_{2K}-FTS_4	26.12	0.15	1.43
PEG_{5K}-FTS_2	17.61	0.13	0.34
PEG_{5K}-FTS_4	26.80	0.12	0.29

[a]Measured by dynamic light scattering particle sizer. [b]PDI = polydispersity index. [c]CMC = critical micelle concentration.

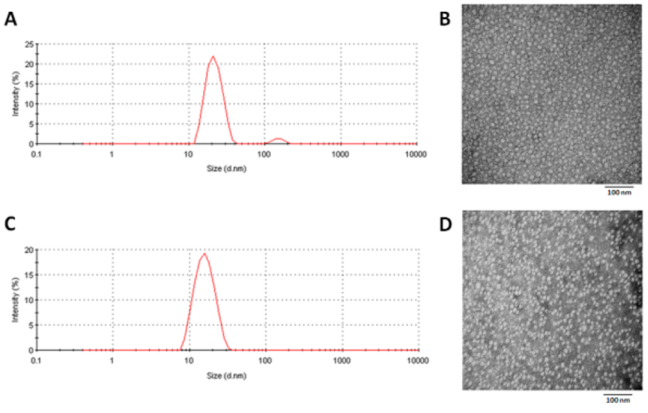

Figure 2. Particle size distribution and morphology of drug-free and PTX-loaded PEG_{5K}-FTS_4 micelles. The size and size distribution of drug-free PEG_{5K}-FTS_4 micelles (A) and PTX-loaded PEG_{5K}-FTS_4 micelles (C) were evaluated by DLS. The morphology of drug-free PEG_{5K}-FTS_4 micelles (B) and PTX-loaded PEG_{5K}-FTS_4 micelles (D) was examined by TEM. The PTX concentration was kept at 1 mg/mL.

Critical Micelle Concentration (CMC). The CMC of PEG_{2K}-FTS_2, PEG_{2K}-FTS_4, PEG_{5K}-FTS_2, and PEG_{5K}-FTS_4 micelles were measured using pyrene as a fluorescence probe (Table 1). When the concentration of the PEG-FTS reached the CMC, the fluorescence intensity of pyrene would change dramatically due to the transfer of pyrene from polar microenvironment to nonpolar surroundings caused by the formation of micelles. The CMCs of PEG_{5K}-FTS_2 and PEG_{5K}-FTS_4 conjugates were determined to be 0.34 and 0.29 μM, respectively, which were lower than those of PEG_{2K}-FTS_2 (1.22 μM) and PEG_{2K}-FTS_4 (1.43 μM) (Supporting Information Figure S5). The lower CMCs of PEG_{5K}-FTS micelles may be attributed to the longer PEG hydrophilic chain and more effective stabilizing effect for the micelles.

Drug Loading. The PTX loading of PEG_{2K}-FTS_2, PEG_{2K}-FTS_4, PEG_{5K}-FTS_2, and PEG_{5K}-FTS_4 micelles with different carrier to drug molar ratios was determined by HPLC (Table 2). The sizes of these PTX loaded PEG-FTS micelles were also evaluated under corresponding conditions. PEG_{5K}-FTS_4 micelles could effectively solubilize PTX in aqueous solution at a molar ratio as low as 1:1 (m/m) with particle size around 50 nm (Table 2). However, these PTX-loaded PEG_{5K}-FTS_4 micelles were only stable for 2.5 h. With an increase in carrier/drug ratio to 2.5/1, they formed mixed micelles with PTX that were stable for about 1 day. For the other three micelles, a minimal carrier/drug ratio of 2.5/1 was required to solubilize PTX. Overall, the conjugates with four molecules of FTS worked better than the conjugates with two molecules of FTS and PEG_{5K} conjugates were more effective than the PEG_{2K}

Table 2. Physicochemical characterization of PTX-loaded PEG-FTS micelles

carrier/PTX ratio	PTX loaded micelles[a]	size[b] (nm)	PDI[c]	DLC[d] (%)	DLE[e] (%)	stability[f] (hours)
1:1	PEG_{2K}-FTS_2/PTX	precipitate				
	PEG_{2K}-FTS_4/PTX	precipitate				
	PEG_{5K}-FTS_2/PTX	precipitate				
	PEG_{5K}-FTS_4/PTX	54.40	0.13	6.6	60.2	2.5
2.5:1	PEG_{2K}-FTS_2/PTX	29.27	0.09	8.2	76.8	1.5
	PEG_{2K}-FTS_4/PTX	42.55	0.24	6.4	80.2	3
	PEG_{5K}-FTS_2/PTX	24.90	0.35	4.5	81.2	2
	PEG_{5K}-FTS_4/PTX	28.16	0.17	4.0	85.6	20
5:1	PEG_{2K}-FTS_2/PTX	28.68	0.09	5.0	89.2	5
	PEG_{2K}-FTS_4/PTX	25.60	0.11	3.8	90.6	28
	PEG_{5K}-FTS_2/PTX	25.63	0.23	2.8	97.6	20
	PEG_{5K}-FTS_4/PTX	26.52	0.08	2.3	94.2	48

[a]PTX concentration in micelles was kept at 1 mg/mL. [b]Measured by dynamic light scattering particle sizer. [c]PDI = polydispersity index. [d]DLC = drug loading capacity. [e]DLE = drug loading efficiency. [f]Data mean that there was no noticeable size change during the follow-up period.

dx.doi.org/10.1021/mp500181x | Mol. Pharmaceutics 2014, 11, 2807−2814

counterparts in forming stable drug loaded micelles. The four conjugates were ranked as PEG_{5K}-FTS_4 > PEG_{2K}-FTS_4 > PEG_{5K}-FTS_2 > PEG_{2K}- FTS_2 with respect to their efficiency in forming stable mixed micelles with PTX.

***In Vitro* PTX Release Study.** The profile of PTX release from the four PEG-FTS micelles was examined by a dialysis method. As shown in Figure 3, PEG_{5K}-FTS_4/PTX mixed micelles showed relatively slower kinetics of PTX release compared to other PTX-loaded PEG-FTS micelles.

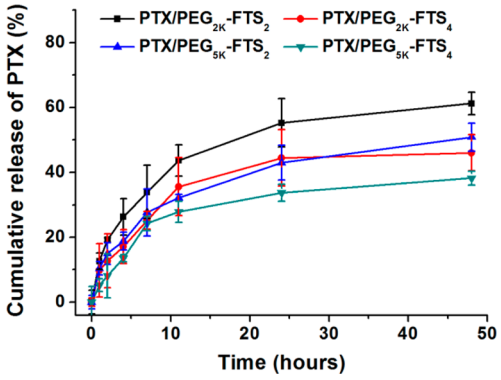

Figure 3. Cumulative PTX release profile from four PTX-loaded PEG-FTS micelles. PBS containing 0.5% (w/v) Tween 80 was used as the release medium. PTX concentration was fixed at 0.5 mg PTX/mL. Values reported are the means ± SD for triplicate samples.

Hemolytic Effect of Micelles. As a delivery system for intravenous application, the potential detrimental interaction of PEG-FTS-based micellar system with blood components should be minimized. Figure 4 shows the hemolytic activities

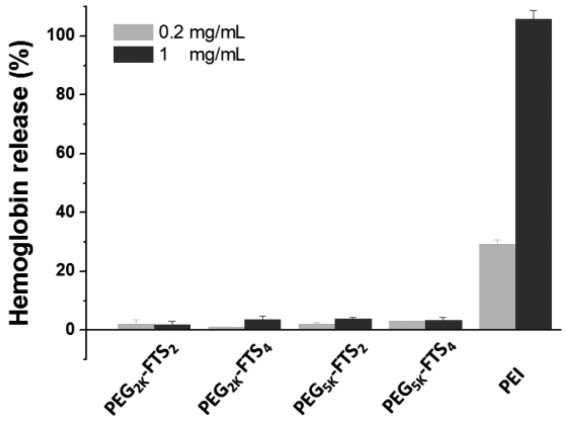

Figure 4. *In vitro* hemolysis assay of four PEG-FTS micelles compared with PEI. Rat RBCs were treated with the four different PEG-FTS micelles or PET at 0.2 and 1 mg/mL, respectively. The lysis of RBCs was determined by measuring the release of hemoglobin spectrophotometrically (λ = 540 nm). RBCs incubated with PBS and Triton X-100 (2%) were used as the negative and positive controls. Values reported are the means ± SD for triplicate samples.

of drug-free PEG_{2K}-FTS_2, PEG_{2K}-FTS_4, PEG_{5K}-FTS_2, and PEG_{5K}-FTS_4 micelles. Polyethylenimine (PEI), a cationic polymer known to have significant hemolytic effect,[30] was included as a positive control. PEI induced hemolysis in a concentration-dependent manner. In contrast, all of the four drug-free PEG-FTS micelles displayed only negligible levels of hemolytic activities, suggesting that PEG-FTS micelles are mild surfactants suitable for *in vivo* delivery of hydrophobic anticancer drugs.

***In Vitro* Cytotoxicity.** Figure 5A shows the cytotoxicity of 4 carriers alone in MCF-7 cells. The FTS_2 conjugates (PEG_{2K}-FTS_2 and PEG_{5K}-FTS_2) were more effective than FTS_4 conjugates (PEG_{2K}- FTS_4 and PEG_{5K}-FTS_4) in inhibiting the tumor cell proliferation. Similar results were found when the four conjugates were examined in HCT-116 (Figure 5B) and 4T1.2 cells (Figure 5C).

Western Blotting. Figure 6 shows the protein expression level of total Ras 20 h following treatment of HCT-116 cells with the four different conjugates at a FTS concentration of 40 μM. Downregulation of Ras protein expression was seen in all treatment groups. However, the conjugates with two FTS molecules were more active than the counterparts with four FTS molecules in reducing the protein expression levels of Ras in HCT-116 cells.

***In Vitro* Cytotoxicity of PTX-Loaded Micelles.** Figure 7 shows the cytotoxicity of free PTX (in DMSO) and PTX formulated in PEG_{2K}-FTS_2, PEG_{2K}-FTS_4, PEG_{5K}-FTS_2 and PEG_{5K}-FTS_4 micelles in 4T1.2 cell line. Free PTX inhibited the cell growth in a dose-dependent manner. Delivery of PTX via the four different PEG-FTS micelles led to varied levels of improvement. Nonetheless, PTX-loaded PEG_{5K}-FTS_4 micelles were more potent than PTX formulated in the other micellar formulations (PEG_{2K}-FTS_2, PEG_{2K}-FTS_4, and PEG_{5K}-FTS_2) in inhibiting the tumor cell growth. The IC_{50} of free PTX and the four micellar formulations of PTX are summarized in Supporting Information Table S1.

***In Vivo* Therapeutic Study.** The *in vivo* therapeutic effectiveness of PTX formulated in PEG_{2K}-FTS_2, PEG_{2K}-FTS_4, PEG_{5K}-FTS_2, and PEG_{5K}-FTS_4 micelles was evaluated, respectively, in a syngeneic murine breast cancer model (4T1.2), and compared to Taxol. As shown in Figure 8A, PTX-loaded PEG_{2K}-FTS_2 micelles exhibited a similar tumor growth inhibitory effect compared to Taxol treatment group. In contrast, PTX formulated in PEG_{5K}-FTS_2 and PEG_{5K}-FTS_4 micelles demonstrated a significantly enhanced antitumor activity compared to Taxol ($P < 0.01$). Furthermore, PTX formulated in PEG_{5K}-FTS_4 showed a trend of improvement in antitumor activity compared with PTX formulated in PEG_{5K}-FTS_2 ($P = 0.09$). No significant changes in body weight were noticed in all treatment groups compared to PBS control group (Figure 8B). In addition, serum levels of transaminases in the mice with different treatments were comparable to those in PBS control group (Table 3).

■ DISCUSSION

We have systematically compared the physicochemical property and the *in vitro* and *in vivo* PTX delivery efficiency of four PEG-FTS conjugates that vary in the length of PEG motif (PEG_{2K} vs PEG_{5K}) and the molar ratio of PEG/FTS (1/2 vs 1/4). All of the four PEG-FTS micelles possessed very small sizes of 20−30 nm. After drug loading, micelles retained small size of 20−60 nm. Doxil (doxorubicin HCl liposome) and Abraxane (albumin-bound paclitaxel) are two FDA-approved formulations. The particle sizes of Doxil and Abraxane are ~150 and 130 nm, respectively. Their relatively large sizes may limit the diffusion in the tumor, and thus limit their therapeutic effectiveness.[32] It has been reported that nanoparticles need to be smaller than 100 nm in order to circumvent macrophage clearance in the lungs[31] and that particles of further reduced size (≤64 nm) are needed for effective penetration through

dx.doi.org/10.1021/mp500181x | *Mol. Pharmaceutics* 2014, 11, 2807−2814

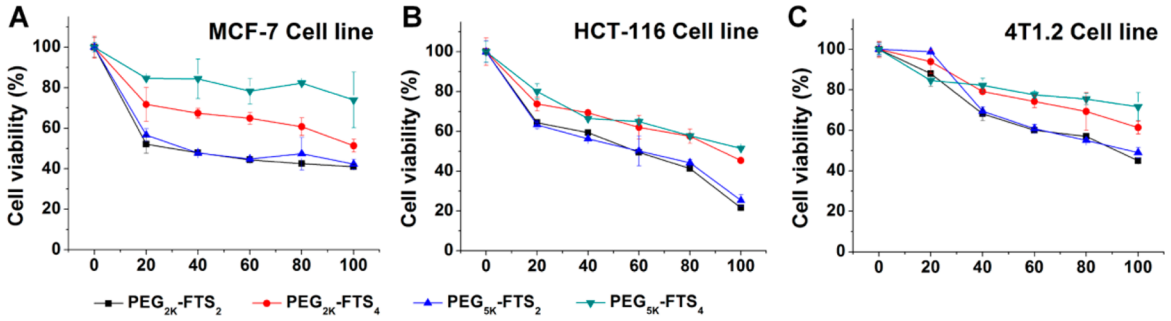

Figure 5. Cytotoxicity of four drug-free PEG-FTS micelles in MCF-7 human breast carcinoma cell line (A), HCT-116 human colon carcinoma cell line (B), and 4T1.2 mouse breast cancer cell line (C). Cells were treated with different micelles for 72 h and cytotoxicity was determined by MTT assay. Values reported are the means ± SD for triplicate samples.

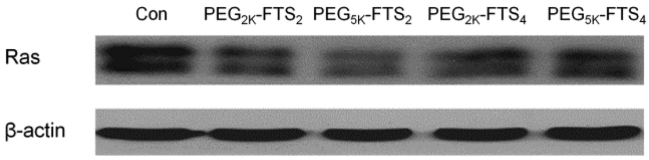

Figure 6. Effects of PEG-FTS micelles on total Ras protein expression in HCT-116 cells. HCT-116 cells were treated with four different PEG-FTS micelles for 20 h (at a FTS concentration of 40 μM). The protein expression level of total Ras was examined by Western blotting.

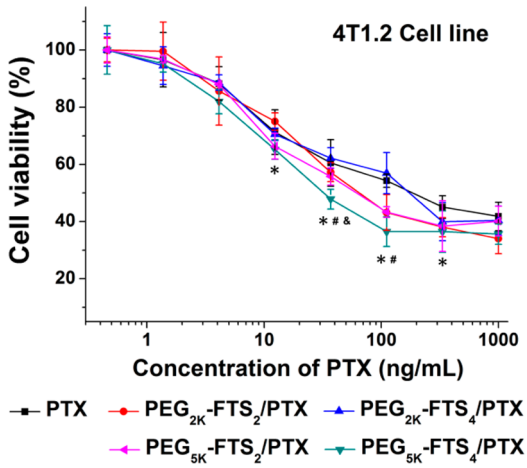

Figure 7. Cytotoxicity of PTX-loaded PEG-FTS micelles in 4T1.2 mouse breast cancer cell line. Cells were treated with free PTX or different micellar formulations of PTX for 72 h and cytotoxicity was determined by MTT assay. PTX-loaded PEG_{5K}-FTS_4 micelles showed an improvement in cell growth inhibition compared with other formulations. $^{*}P < 0.05$ (PTX/PEG_{5K}-FTS_4 vs PTX), $^{\#}P < 0.05$ (PTX/PEG_{5K}-FTS_4 vs PTX/PEG_{5K}-FTS_2 or PTX/PEG_{2K}-FTS_4), $^{\&}P < 0.05$ (PTX/PEG_{5K}-FTS_4 vs PTX/PEG_{2K}-FTS_2, PTX/PEG_{5K}-FTS_2, or PTX/PEG_{2K}-FTS_4). Values reported are the means ± SD for triplicate samples.

neovasculatures to reach tumor cells.[10,11] The small sizes of our PEG-FTS micelles shall ensure efficient passive targeting to the solid tumors.

In addition to size, drug loading capacity and formulation stability are two other important features for an effective micellar system. Our data showed that the PEG-FTS conjugates with four FTS molecules were significantly more effective than the conjugates with two molecules of FTS in forming stable drug-loaded micelles. Previous studies have shown that increasing the ratio of hydrophobic/hydrophilic blocks is associated with increased drug loading capacity and enhanced formulation stability.[22] The improved performance of PEG-FTS conjugates with an increased number of core forming units may be attributed to a similar mechanism. FTS, as a hydrophobic core of micelles, has a lipid chain and benzene ring structure. The lipid chain of FTS contributes to the loading of hydrophobic drug through hydrophobic interaction. At the same time, the benzene ring of FTS is capable of forming $\pi-\pi$ interaction with drug carrying aromatic ring structure. In the PEG-FTS micellar system, $\pi-\pi$ stacking and hydrophobic interaction are likely to work cooperatively to promote both drug/carrier and carrier/carrier interactions. Such interactions are also expected to be further enhanced with an increase in the number of FTS molecules in PEG-FTS conjugates.

PEG is widely used as a polymeric steric stabilizer. A prominent advantage of PEG modification is to impart the *in vivo* longevity to drug carriers. Torchilin's group[33] has reported that PEG/core ratio affected the performance of the micelles. Furthermore, the length of PEG also acted on the CMC, which in turn influenced the performance of the micelles, particularly *in vivo*.[22,24,26] Our data showed that PEG_{5K}-conjugates had a lower CMC and were more effective than PEG_{2K}-conjugates in forming stable micelles with PTX.

One unique feature for PEG-FTS micellar delivery system is its intrinsic antitumor activity. The four different PEG-FTS conjugates showed varied levels of antitumor activity by themselves in three cancer cell lines. The conjugates with two FTS molecules showed higher levels of cytotoxicity compared to the counterparts with four FTS molecules. The higher levels of cytotoxicity for the conjugates with two FTS molecules are unlikely due to a more active surface activity of the double chain conjugates as all of the four conjugates showed minimal hemolytic activity (Figure 4). It is likely that active FTS is more readily cleaved from the conjugates with two FTS than the ones with four FTS molecules due to less steric hindrance to intracellular esterases. We also compared the *in vitro* cytotoxicity of the four PTX-loaded PEG-FTS micelles (Figure 7). PTX-loaded PEG_{5K}-FTS_4 micelles showed better cytotoxicity than free PTX and PTX formulated in other three micelles in 4T1.2 cells. This is likely due to a more efficient intracellular delivery of PTX via PEG_{5K}-FTS_4 micelles because PEG_{5K}-FTS_4 formed the most stable micelles with PTX among the four micellar systems tested.

In vivo therapy study clearly showed a significantly higher level of antitumor activity for PTX formulated in PEG_{5K}-FTS_4 micelles compared to either Taxol or PTX formulated in PEG_{2K}-FTS_2 (Figure 8A). This is likely due to the significantly

dx.doi.org/10.1021/mp500181x | *Mol. Pharmaceutics* 2014, 11, 2807−2814

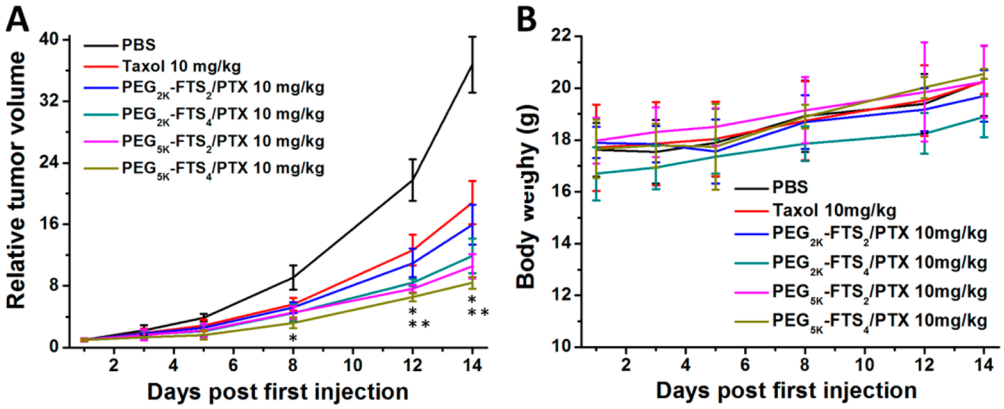

Figure 8. Enhanced antitumor efficacy of PTX loaded in PEG_{5K}-FTS_4 micelles. BABL/c mice were inoculated s.c. with 4T1.2 cells (2×10^5 cells/mouse). Six days later, mice received various treatments twice a week and tumor growth was monitored and plotted as relative tumor volume (A). Significant improvement in antitumor activity was found for the PTX-loaded PEG_{5K}-FTS_4 group compared with the Taxol group (**$P < 0.01$; $N = 5$) and the group of PTX-loaded PEG_{2K}-FTS_2 (*$P < 0.05$; $N = 5$). Changes in body weights of mice in different treatment groups were also monitored (B).

Table 3. Serum Levels of Transaminases in Mice of Different Treatment Groups

groups	ALT[a] (U/L)	AST[b] (U/L)
PBS	37.3 ± 1.0	94.3 ± 20.4
Taxol (10 mg/kg)	22.2 ± 4.1	97.6 ± 1.4
PEG_{2K}-FTS_2/PTX (10 mg/kg)	23.2 ± 1.7	102.6 ± 15.9
PEG_{2K}-FTS_4/PTX (10 mg/kg)	26.4 ± 1.0	94.3 ± 36.4
PEG_{5K}-FTS_2/PTX (10 mg/kg)	22.2 ± 0.7	86.3 ± 11.5
PEG_{5K}-FTS_4/PTX (10 mg/kg)	24.0 ± 2.8	130.3 ± 28.8

[a]ALT = alanine aminotransferase. [b]AST = aspartate aminotransferase.

improved stability for PEG_{5K}-FTS_4 micelles, which contributes to more effective delivery of PTX to tumor tissue *in vivo*.

CONCLUSIONS

In summary, we have shown that PEG_{5K}-FTS_4 formed the most stable mixed micelles with PTX among four PEG-FTS micelles. Furthermore, PTX formulated in PEG_{5K}-FTS_4 micelles was more active in cytotoxicity than free PTX and PTX formulated in other three PEG-FTS micelles. *In vivo*, PTX-loaded PEG_{5K}-FTS_4 led to an improved tumor growth inhibitory effect in comparison to PTX formulated in PEG_{2K}-FTS_2, PEG_{2K}-FTS_4, and PEG_{5K}-FTS_2 as well as Taxol in a syngeneic mouse model of breast cancer (4T1.2). More studies on the structure and activity relationship are needed to further improve the PEG-FTS-based delivery system.

ASSOCIATED CONTENT

Supporting Information

IC_{50} data, 1H NMR spectra, MALDI−TOF, size distribution, TEM, and critical micelle concentration of the conjugates. This material is available free of charge via the Internet at http://pubs.acs.org.

AUTHOR INFORMATION

Corresponding Author

*S. Li. E-mail: sol4@pitt.edu. Tel.: 412-383-7976. Fax: 412-648-1664. Address: Center for Pharmacogenetics, Department of Pharmaceutical Sciences, University of Pittsburgh School of Pharmacy, 639 Salk Hall, Pittsburgh, PA 15261, United States.

Notes

The authors declare no competing financial interest.

ACKNOWLEDGMENTS

We would like to thank Drs. Donna Stolz and Ming Sun for their help with TEM study. This work was supported in part by NIH grants R21CA173887, RO1CA174305, and R01GM102989.

REFERENCES

(1) Kumar, N. Taxol-induced polymerization of purified tubulin. Mechanism of action. *J. Biol. Chem.* **1981**, *256*, 10435−10441.
(2) Weiss, R. B.; Donehower, R. C.; Wiernik, P. H.; Ohnuma, T.; Gralla, R. J.; Trump, D. L.; Baker, J. R.; Van Echo, D. A.; Von Hoff, D. D.; Leyland-Jones, B. Hypersensitivity reactions from taxol. *J. Clin. Oncol.* **1990**, *8*, 1263−1268.
(3) Nishiyama, N.; Kataoka, K. Current state, achievements, and future prospects of polymeric micelles as nanocarriers for drug and gene delivery. *Pharmacol. Ther.* **2006**, *112*, 630−648.
(4) Kataoka, K.; Harada, A.; Nagasaki, Y. Block copolymer micelles for drug delivery: design, characterization and biological significance. *Adv. Drug Delivery Rev.* **2012**, *47*, 113−131.
(5) Adams, M. L.; Lavasanifar, A.; Kwon, G. S. Amphiphilic block copolymers for drug delivery. *J. Pharm. Sci.* **2003**, *92*, 1343−1355.
(6) Torchilin, V. P. Micellar nanocarriers: pharmaceutical perspectives. *Pharm. Res.* **2007**, *24*, 1−16.
(7) Wei, H.; Zhuo, R. X.; Zhang, X. Z. Design and development of polymeric micelles with cleavable links for intracellular drug delivery. *Prog. Polym. Sci.* **2013**, *38*, 503−535.
(8) Perrault, S. D.; Walkey, C.; Jennings, T.; Fischer, H. C.; Chan, W. C. Mediating tumor targeting efficiency of nanoparticles through design. *Nano Lett.* **2009**, *9*, 1909−1915.
(9) Maeda, H.; Wu, J.; Sawa, T.; Matsumura, Y.; Hori, K. Tumor vascular permeability and the EPR effect in macromolecular therapeutics: a review. *J. Controlled Release* **2000**, *65*, 271−284.
(10) Luo, J.; Xiao, K.; Li, Y.; Lee, J. S.; Shi, L.; Tan, Y. H.; Xing, L.; Cheng, R. H.; Liu, G. Y.; Lam, K. S. Well-defined, size-tunable, multifunctional micelles for efficient paclitaxel delivery for cancer treatment. *Bioconjugate Chem.* **2010**, *21*, 1216−1224.
(11) Cabral, H.; Matsumoto, Y.; Mizuno, K.; Chen, Q.; Murakami, M.; Kimura, M.; Terada, Y.; Kano, M. R.; Miyazono, K.; Uesaka, M.; Nishiyama, N.; Kataoka, K. Accumulation of sub-100 nm polymeric micelles in poorly permeable tumours depends on size. *Nat. Nanotechnol.* **2011**, *6*, 815−823.
(12) Zhang, X.; Huang, Y.; Li, S. Nanomicellar carriers for targeted delivery of anticancer agents. *Ther. Delivery* **2014**, *5*, 53−68.

(13) Bourzac, K. Nanotechnology: Carrying drugs. *Nature* **2012**, *491*, S58−60.
(14) Zhang, X.; Lu, J.; Huang, Y.; Zhao, W.; Chen, Y.; Li, J.; Gao, X.; Venkataramanan, R.; Sun, M.; Stolz, D. B.; Zhang, L.; Li, S. PEG-farnesylthiosalicylate conjugate as a nanomicellar carrier for delivery of paclitaxel. *Bioconjugate Chem.* **2013**, *24*, 464−472.
(15) Mor, A.; Aizman, E.; Chapman, J.; Kloog, Y. Immunomodulatory properties of farnesoids: the new steroids? *Curr. Med. Chem.* **2013**, *20*, 1218−24.
(16) Baines, A. T.; Xu, D.; Der, C. J. Inhibition of Ras for cancer treatment: the search continues. *Future Med. Chem.* **2011**, *3*, 1787−1808.
(17) Haklai, R.; Weisz, M. G.; Elad, G.; Paz, A.; Marciano, D.; Egozi, Y.; Ben-Baruch, G.; Kloog, Y. Dislodgment and accelerated degradation of Ras. *Biochemistry* **1998**, *37*, 1306−1314.
(18) Rotblat, B.; Ehrlich, M.; Haklai, R.; Kloog, Y. The Ras inhibitor farnesylthiosalicylic acid (Salirasib) disrupts the spatiotemporal localization of active Ras: a potential treatment for cancer. *Methods Enzymol.* **2008**, *439*, 467−489.
(19) Jansen, B.; Schlagbauer-Wadl, H.; Kahr, H.; Heere-Ress, E.; Mayer, B. X.; Eichler, H.; Pehamberger, H.; Gana-Weisz, M.; Ben-David, E.; Kloog, Y.; Wolff, K. Novel Ras antagonist blocks human melanoma growth. *Proc. Natl. Acad. Sci. U. S. A.* **1996**, *96*, 14019−14024.
(20) Niv, H.; Gutman, O.; Henis, Y. I.; Kloog, Y. Membrane interactions of a constitutively active GFP-Ki-Ras 4B and their role in signaling. Evidence from lateral mobility studies. *J. Biol. Chem.* **1999**, *274*, 1606−1613.
(21) Kloog, Y.; Cox, A. D.; Sinensky, M. Concepts in Ras-directed therapy. *Expert Opin. Invest. Drugs* **1999**, *8*, 2121−2140.
(22) Lu, J.; Huang, Y.; Zhao, W.; Chen, Y.; Li, J.; Gao, X.; Venkataramanan, R.; Li, S. Design and characterization of PEG-derivatized vitamin E as a nanomicellar formulation for delivery of paclitaxel. *Mol. Pharmacol.* **2013**, *10*, 2880−90.
(23) Wang, J.; Sun, J.; Chen, Q.; Gao, Y.; Li, L.; Li, H.; Leng, D.; Wang, Y.; Sun, Y.; Jing, Y.; Wang, S.; He, Z. Star-shape copolymer of lysine-linked di-tocopherol polyethylene glycol 2000 succinate for doxorubicin delivery with reversal of multidrug resistance. *Biomaterials* **2012**, *33*, 6877−88.
(24) Mi, Y.; Liu, Y.; Feng, S. S. Formulation of Docetaxel by folic acid-conjugated d-alpha-tocopheryl polyethylene glycol succinate 2000 (Vitamin E TPGS(2k)) micelles for targeted and synergistic chemotherapy. *Biomaterials* **2011**, *32*, 4058−66.
(25) Huang, Y.; Lu, J.; Gao, X.; Li, J.; Zhao, W.; Sun, M.; Stolz, D. B.; Venkataramanan, R.; Rohan, L. C.; Li, S. PEG-derivatized embelin as a dual functional carrier for the delivery of paclitaxel. *Bioconjugate Chem.* **2012**, *23*, 1443−1451.
(26) Lu, J.; Huang, Y.; Zhao, W.; Marquez, R. T.; Meng, X.; Li, J.; Gao, X.; Venkataramanan, R.; Wang, Z.; Li, S. PEG-derivatized embelin as a nanomicellar carrier for delivery of paclitaxel to breast and prostate cancers. *Biomaterials* **2013**, *34*, 1591−1600.
(27) Marciano, D.; Ben-Baruch, G.; Marom, M.; Egozi, Y.; Haklai, R.; Kloog, Y. Selective inhibition of Ras-dependent cell growth by farnesylthiosalicylic acid. *J. Med. Chem.* **1995**, *38*, 1267−1272.
(28) Duan, K.; Zhang, X. L.; Tang, X. X.; Yu, J. H.; Liu, S. Y.; Wang, D. X.; Li, Y. L.; Huang, J. Fabrication of cationic nanomicelle from chitosan-graft-polycaprolactone as the carrier of 7-ethyl-10-hydroxy-camptothecin. *Colloids Surf., B* **2010**, *76*, 475−482.
(29) Xiao, K.; Li, Y.; Luo, J.; Lee, J. S.; Xiao, W.; Gonik, A. M.; Agarwal, R. G.; Lam, K. S. The effect of surface charge on *in vivo* biodistribution of PEG-oligocholic acid based micellar nanoparticles. *Biomaterials* **2011**, *32*, 3435−3446.
(30) Reul, R.; Nguyen, J.; Kissel, T. Amine-modified hyperbranched polyesters as non-toxic, biodegradable gene delivery systems. *Biomaterials* **2009**, *30*, 5815−5824.
(31) Wiebert, P.; Sanchez-Crespo, A.; Seitz, J.; Falk, R.; Philipson, K.; Kreyling, W. G.; Möller, W.; Sommerer, K.; Larsson, S.; Svartengren, M. Negligble clearance of ultrafine particles retained in healthy and affected human lungs. *Eur. Respir. J.* **2006**, *28*, 286−290.
(32) Dreher, M. R.; Liu, W.; Michelich, C. R.; Dewhirst, M. W.; Yuan, F.; Chilkoti, A. Tumor vascular permeability, accumulation, and penetration of macromolecular drug carriers. *J. Natl. Cancer Inst.* **2006**, *98*, 335−44.
(33) Sawant, R. R.; Torchilin, V. P. Multifunctionality of lipid core micelles for drug delivery and tumor targeting. *Mol. Membr. Biol.* **2010**, *27*, 232−246.